United Nations Scientific Committee on the Effects of Atomic Radiation

ATTACHMENT F-2

TERRESTRIAL ECOSYSTEM APPLICATION OF ASSESSMENT METHODS AND LIFE HISTORY

UNSCEAR 2013 Report, Annex A, Levels and effects of radiation exposure due to the nuclear accident after the 2011 great east-Japan earthquake and tsunami, Appendix F (Assessment of doses and effects for non-human biota)

Notes

The designations employed and the presentation of material in this publication do not imply the expression of any opinion whatsoever on the part of the Secretariat of the United Nations concerning the legal status of any country, territory, city or area, or of its authorities, or concerning the delimitation of its frontiers or boundaries.

© United Nations, August 2014. All rights reserved, worldwide.

This publication has not been formally edited.

Contents

NOTES 1

I. INTRODUCTION 2

II. METHODOLOGY FOR THE DETAILED ASSESSMENT AT SITES WHERE DIRECT MEASUREMENTS IN ANIMALS WERE AVAILABLE 3

III. EQUILIBRIUM ASSESSMENTS 10

IV. SETTING UP THE DYNAMIC MODEL 12

V. RESULTS 13

REFERENCES 19

I. INTRODUCTION

1. The assessment for the terrestrial system covers three of the main steps outlined in the generic methodology (see attachment F-1; Introduction):

a. Focus was initially placed upon the locations where direct measurements in terrestrial animals were available. Combining a spatial analysis of deposition density data with cluster analyses of activity concentrations in biota resulted in the most reliable estimation of dose rates for the selected animals at the time of sampling;

b. An equilibrium assessment for locations where no direct measurements of activity concentrations in biota were available was performed. Focus was placed on an area of maximum deposition density to provide an upper percentile (and thus conservative) estimate on exposures of plants and animals in the accident-affected region at the time of the deposition density measurement. Further calculations were made to account for the decay of short-lived radionuclides to provide an estimate for exposures at the time of maximum deposition density.

c. A dynamic assessment was conducted to further explore the time evolution of concentration levels in plants and animals. Predictions of ^{137}Cs activity concentrations in vegetation and deer/herbivorous mammal were made, and the latter values were compared against empirical datasets for Sika deer. The model was applied to the area of maximum deposition density (as in b above) to provide further refinement through insight into the temporal evolution of concentration levels at sites of relatively high deposition density.

II. METHODOLOGY FOR THE DETAILED ASSESSMENT AT SITES WHERE DIRECT MEASUREMENTS IN ANIMALS WERE AVAILABLE

2. The initial stage of the assessment required interpolation of deposition density data between measurement points. This was required subsequently to predict deposition levels at locations where biota had been sampled and, where appropriate, to average deposition density levels over the home range of the animal, thus facilitating the derivation of concomitant average external dose rates.

(a) Empirical Bayesian Kriging (EBK)

3. Empirical Bayesian Kriging was selected as the method to calculate the ^{137}Cs and ^{134}Cs deposition density rasters for the Fukushima area. This method estimates values based on semivariogram models that are derived from the input data. Empirical Bayesian Kriging uses Bayes' rule to estimate the optimum weight for the 'local' semivariograms [Krivoruchko, 2011; Gribov & Krivoruchko, 2012; Pilz et al., 2012].

4. Error estimates were modelled by running the EBK prediction on a randomly split dataset (95% of the data) and then comparing the modelled value with the measured value using the remaining 5%. This was repeated 20 times. The resulting error (absolute percentage difference) is shown as a histogram (figure I).

Figure I. Histogram showing error (absolute % difference) between EBK predicted and measured ^{137}Cs deposition density data

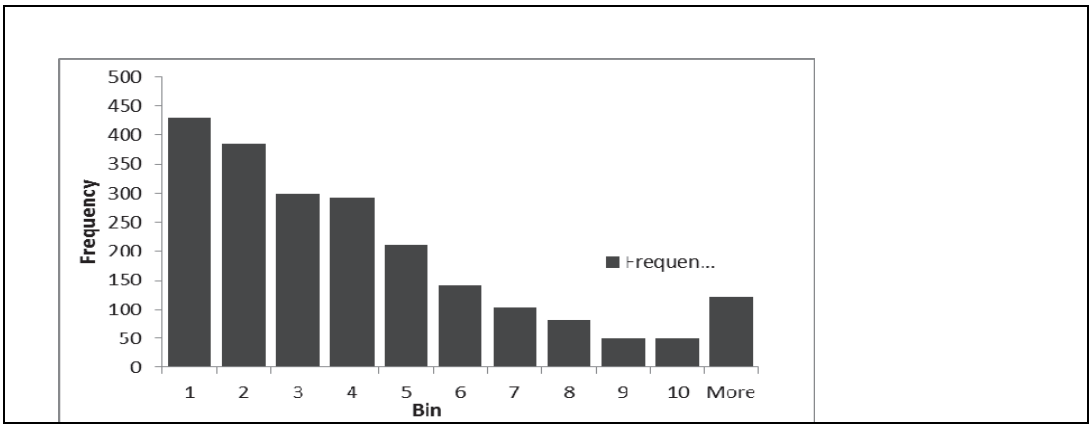

5. The coordinate system for the spatial analysis was WGS84 UTM zone 54n. The deposition raster for ^{137}Cs is presented in figure II and for ^{134}Cs in figure III.

Figure II. Deposition density of ^{137}Cs (kBq/m^2)

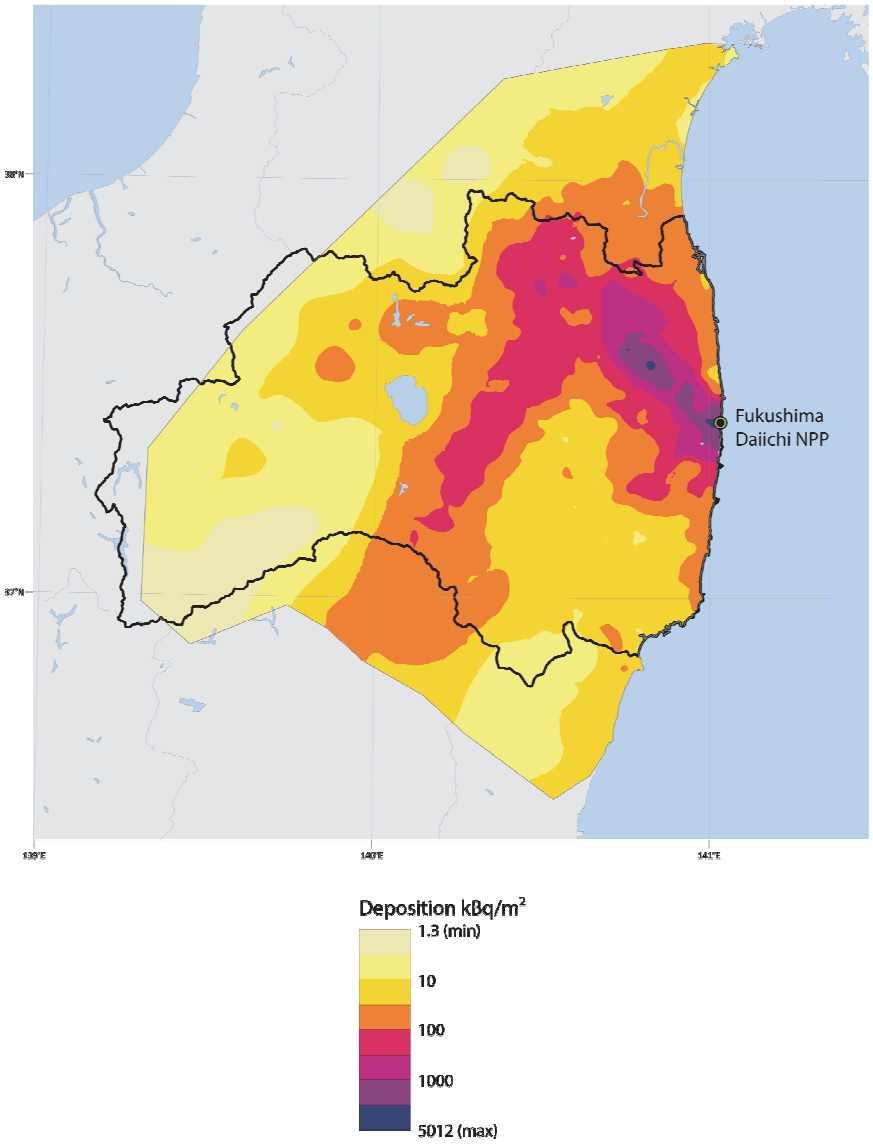

Figure III. Deposition density of ^{134}Cs (kBq/m^2)

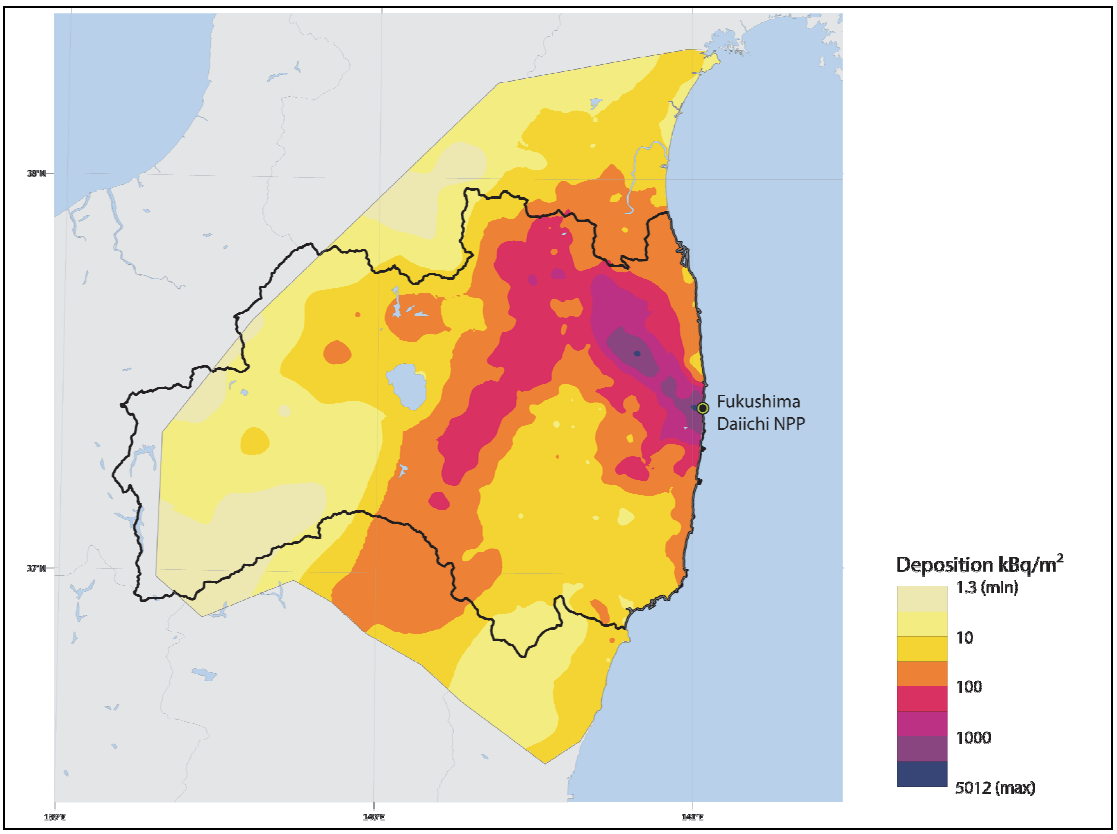

6. With regard to data for biota, measured activity concentrations for ^{131}I, ^{134}Cs and ^{137}Cs in mammals and birds were available. These data sets contained additional information, such as weight, length, age and sex of measured biota. Table 1 provides an overview of the biota data.

Table 1. List of animal species and concomitant information from datasets provided by Fukushima Prefecture [2013]

Organism	*Latin name*	*Nr. of data*	*Data*	
			Weight (kg)	*Length (cm)*
Wild boar	*Sus scrofa*	153	10–150 (55)*	30–160 (101)*
Asian black bear	*Ursus thibetanus*	19	50–140 (72)*	100–160 (120)*
Sika deer	*Cervus Nippon*	10	60–120 (72)*	100–160 (139)*
Common teal	*Anas crecca*	1	1	20
Copper pheasant	*Symaticus sommerringii*	11	1	90
Grey duck	*Anas poecilorhyncha*	23	1	30–60
Japanese pheasant	*Phasianus versiclor*	35		
Mallard	*Anas platyrhynchos*	8	1	50

*Average values.

7. The first step involved placing all the deposition density and activity concentration data on maps. The spatial distribution of data on radionuclide activity concentration in animals and birds was examined using a Geographical Information System (GIS) and this resulted in the following maps for ^{137}Cs deposition density data (figures IV and V).

Figure IV. ^{137}Cs deposition density with sampling locations of mammals and birds superimposed

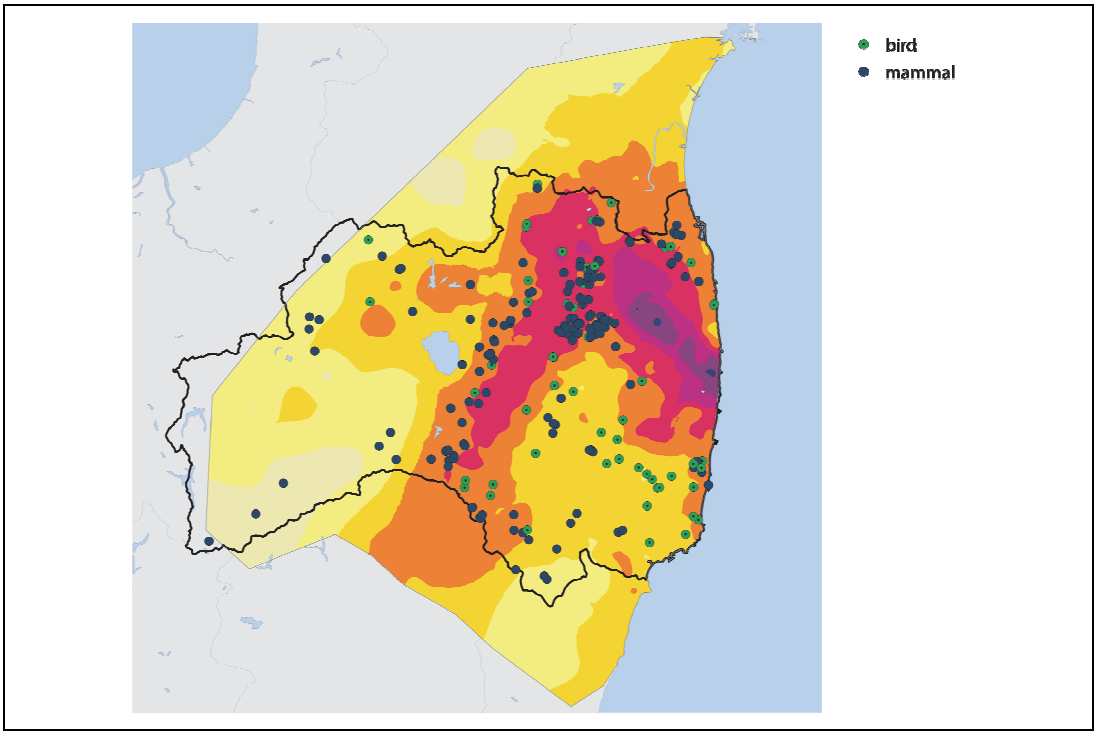

Figure V. ^{137}Cs deposition density data with distribution of mammal species superimposed

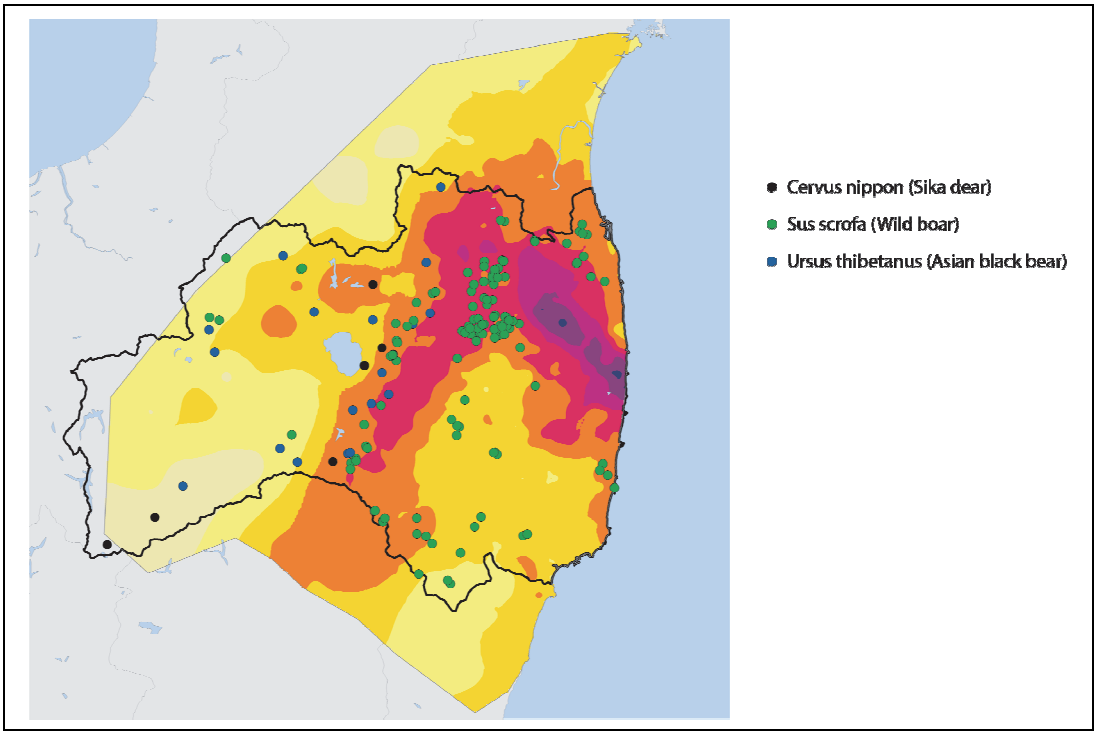

(b) Preparation of data for detailed assessment

8. The plan was to perform a more detailed analysis, preferably using actual radionuclide concentrations in the biota. Initial categorization of data showed that, in fact, there were only three species of mammal and five species of bird (see table 1). Most of the mammal data were for wild boar so there seemed some justification (in view of the limtied number of species covered and weighting of data towards certain species) to treat each species separately. This involved the use of the 'new organism' function in the ERICA Tool [Brown et al., 2008] and creation of geometries which correspond to the species under discussion. This, in turn, involved collection of life history data and thereafter extraction of relevant data for the assessment.

(c) Life history data and derivation of relevant parameters

9. To derive dose conversion coefficients (DCCs), information on mass and dimensions of the organism is needed. Furthermore, information on habitat is needed and, where applicable, the fractional occupancy of various organisms in their habitats. This information is important to weight external dose rates in order to account for the behaviour of the organism.

10. Life history data sheets containing basic ecological information about all organisms involved in the assessment were collated. In addition to the list of organisms considered, table 1 shows a summary of the collected information used to derive DCCs. The assumed tissue density for birds was 0.85 g/cm^3 [Hamershock et al., 1993] and that of the mammal species was 1.0 g/cm^3. For birds, the assumed mass and dimensions were taken from ICRP and correspond to ICRP's "RAP duck". The dimensions of mammals were derived from their mass and density. The approach consisted of three steps. First, the length of the animal was found by examining the available data and also consulting literature. Second, a representative picture of the animal was selected on which width could be measured. Third, the relationship between mass, volume and density was used to estimate the third dimension. Table 2 summarizes all the relevant parameters which were used in deriving DCCs.

11. For wild boar, there were distinct clusters whereas for other mammals and birds, the data were rather "spread out". For the wild boar, life history data were examined to define a home range. This analysis showed that a wild boar's home range changes because of many factors (e.g. food availibility and hunting season). A home range was assumed for further calculations to be represented by a circular area with a radius of 3 km. Then, a circle was overlayed (with radius 3 km, corresponding to the home range) around the midpoint of the cluster (the exact position of which was slightly arbitrarily placed by judgement) and then all depsoition density data within the circle were selected and used to estimate external dose rates.

(d) Sample points clustering — option 1

12. Caesium-134 measurements of wild boar were collected in the Fukushima area. No information about home ranges of the sampled animals was available; therefore, the clusters of sample points were identified by their spatial location only. The method used assumed that points within one cluster were within a certain distance of one other. This distance was set to the nearest observed mean distance for all points in the dataset. Clusters were grown from random seed points in an iterative process. One point could belong to more than one cluster.

Table 2. Dimensions and selected life history data for samples mammals and birds

Organism (no. of samples)	*Literature*		*Data*		*Assumed*				*Home range (km^2)*	*Occupancy factor***
	Weight (kg)	*Length (cm)*	*Weight (kg)*	*Length (cm)*	*Weight (kg)*	*Dimensions (cm)*				
Wild boar (153)	50–90	110–150	10–150 (55)*	30–160 (101)*	55	80	40	33	~26	1 on ground
Asian black bear (19)	Male: 90–150 Female: 65–90	120–195	50–140 (72)*	100–160 (120)*	120	126	45	40	~1	0.85 on ground 0.15 on trees
Sika deer (10)	25–110	105–155	60–120 (72)*	100–160 (139)*	70	103	50	26	~2	1 on ground
Common teal (1)			1	20	1.26#	30#	10#	8#	~4	0.75 on water 0.25 in air
Copper pheasant (11)			1	90	1.26#	30#	10#	8#	~2.6	0.75 on ground 0.25 in air
Grey duck (23)			1	30–60	1.26#	30#	10#	8#	Not large	0.75 on water 0.25 in air
Japanese pheasant (35)	0.7–1.4	25–80			1.26#	30#	10#	8#	~2.6	0.75 on ground 0.25 in air
Mallard (8)			1	50	1.26#	30#	10#	8#	1–3	0.75 on water 0.25 in air

*Average; # "ICRP duck" values.
** For birds, a more conservative occupancy factor would have resulted if 'in air' had been changed to either 'on water' or 'on soil'.

13. The "cluster numbers per point" stabilize after a certain number of iteration steps. The number of iteration steps depends on the number of sampling points in the dataset and the estimated variance [Clarke and Evans, 1954]. For each individual point, a cluster score was kept. The scores were then ranked. The highest scoring cluster number was assigned to the point. The smallest cluster size was two points.

(e) Sample points clustering — option 2

14. For the spatial clustering of the wild boar data, a method was used based upon the "Partitioning around Medoids (PAM)" algorithm [Kaufman and Rousseeuw, 2005]. The algorithm was applied to wild-boar groups with an average home range of 3 km. This information was then used to extract concomitant deposition density data for the derivation of external absorbed dose rates.

Figure VI. Results from cluster analyses: clusters denoted by colours and specific numbers

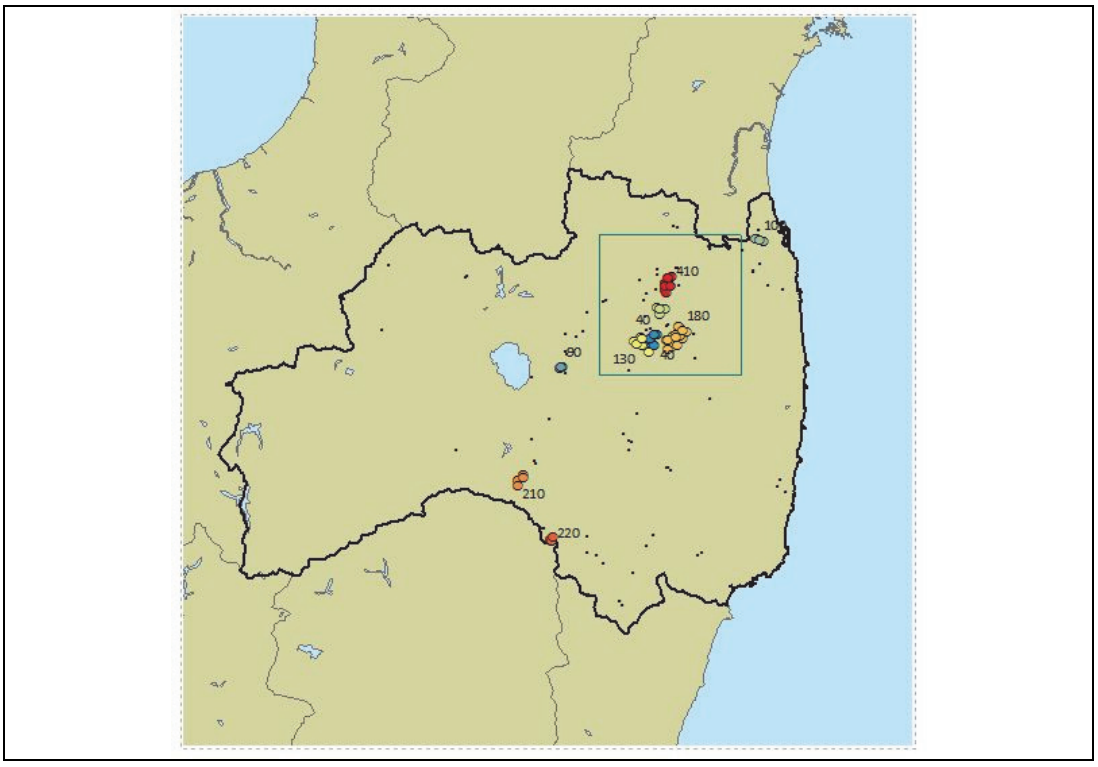

15. In order to extend the information on ^{137}Cs to all other radionuclides, use was made of radionuclide ratios. In essence, the data set for each organism group was used to examine location-specific and generic ratios. The location-specific approach used ratios from the particular area where an animal was sampled, whereas the generic ratios simply related to all available ratio data for that particular animal. The ratios were thus applied to the ^{137}Cs deposition density data to provide information for the poorly characterized radioisotopes (^{110m}Ag, ^{129m}Te, ^{131}I, ^{89}Sr, ^{90}Sr and ^{239}Pu).

III. EQUILIBRIUM ASSESSMENTS

(a) Assessment for sites of relatively high deposition density — data selection and preparation

16. An assessment was conducted in order to indicate the maximum environmental dose rates that could have been encountered in areas where direct measurements on animals and plants were unavailable. The approach adopted was to identify the maximum reported deposition density levels (attachments C-1 to C-7) applying concentration ratios (CRs) to derive whole-body activity concentrations in selected plants and animals. By applying CRs, it was recognized that poor estimates of internal activity concentrations in biota might result, reflecting a lack of suitability in applying these ratios to a system clearly not under equilibrium. Whether the application of CRs in the intermediate phase (i.e. first months) after deposition leads to over-estimation or under-estimation of internal activity concentrations was not immediately evident. On the one hand, a consideration that the rate constants governing transfer of radionuclides from soil through food chains corresponded to half-times in the order of days and weeks led to the inference that substantial time is required for equilibrium to be established. As a consequence, activity concentrations in any given animal needed time to attain levels that would reflect the longer-term, equilibrated partitioning between activity concentrations in animals and soil that CRs are intended to characterize. Thus, applying CRs to soil activity concentrations in the intermediate phase after deposition might have a tendency to over-estimate activity concentrations in animals because the time necessary to allow accumulation in the animals' bodies had not elapsed. On the other hand, radionuclides in the intermediate phase after deposition would be expected to be relatively available for transfer to herbivores because they are present on the surface of vegetation. From such a perspective, the application of terrestrial CRs, based as they are on conditions where root uptake dominates the initial link in radionuclide transfer from soil to the food chain, might be expected to under-estimate activity concentrations in animals. In the absence of direct measurements, these speculations are best resolved through the application of dynamic models.

17. The following approach was adopted for the elevated deposition density, equilibrium-based assessment:

- The sampling location from requested dataset (attachment C-2) that gave the highest deposition density values was selected;
- The maximum and arithmetic mean deposition (Bq/m^2) for the selected location and for all radionuclides were derived (table 3);
- Deposition values were converted to activity concentrations in soil using a generic density of 1300 kg/m^3 [Yasunari et al., 2011] and specified soil depth of 5 cm (table 3);
- These activity concentration data for soil were used as input data to the ERICA Tool using CRs given by ICRP [2009].

Table 3. Radionuclide deposition data for Okuma Town

	^{134}Cs	^{137}Cs	^{89}Sr	^{90}Sr	$^{239,240}Pu$	^{129m}Te	^{110m}Ag	^{131}I
Maximum Deposition (Bq/m^2)	1.40E+07	1.55E+07	6.26E+03	1.46E+03	3.06E+00	2.66E+06	1.36E+04	3.18E+04
Maximum Concentration (Bq/kg)	2.16E+05	2.38E+05	9.63E+01	2.25E+01	4.71E-02	4.10E+04	2.10E+02	4.89E+02
Arithmetic mean deposition (Bq/m^2)	2.49E+06	2.77E+06	3.10E+03	7.25E+02	2.16E+00	5.16E+05	4.89E+03	3.18E+04
Arithmetic mean concentration (Bq/kg)	3.83E+04	4.27E+04	4.77E+01	1.12E+01	3.32E-02	7.94E+03	7.53E+01	4.89E+02
Number of samples	14	14	3	3	3	13	7	1

(b) Input data for an area covering a high variability of deposition – Koriyama City

18. Owing to the limitation of available empirical data, this method (the cluster approach) was not applicable to biota other than wild boar. Therefore, to characterize the exposure situation for other mammals and birds, another approach was taken. Upon closer inspection of the existing datasets, the biota dataset for Koriyama City was found to be the best, because it provided coverage of all considered species. Hence deposition density and activity concentration data for this location were extracted and presented giving minimum, mean and maximum values. The wildlife dataset contained data for five different species of bird, but as their numbers were very few they were pooled under a single category. Table 4 shows the available wildlife data for Koriyama City.

Table 4. Activity concentrations in soil for Koriyama City

Species	^{134}Cs *(Bq/kg)*			^{137}Cs *(Bq/kg)*		
	n	*Mean*	*Range*	*n*	*Mean*	*Range*
Wild boar	12	134	38 – 267	12	156	54 – 289
Asian black bear	2	175	113 – 237	2	201	132 – 270
Sika deer	3	85	63 – 108	3	106	85 – 143
Birds	6	40	22 – 71	8	41	18 – 81

19. A further equilibrium analysis was conducted to account for the radioactive decay of all radionuclides with physical half-lives of less than one year — i.e. ^{131}I, ^{110m}Ag, ^{89}Sr and ^{129m}Te — between the time of sampling and the initial deposition event. According to Yoshida and Takahashi [2012], the main wet deposition events after the Fukushima accident occurred on 15–16 March in the northern Fukushima prefecture. The reference date for most of the radionuclides from Okuma Town was specified as 14 June 2011 (there were several samples with a reference date of 13 June 2011 and one sample, for which the ^{131}I value was reported of 20 June 2011). The reference date of 14 June 2011 was used in all calculations giving an elapsed time between the main deposition event and sampling/measurement of 90 days for decay correction.

20. The IAEA [2010] noted that CRs based on data pertaining to stable elements (or radionuclides with relatively long physical half-lives) should be modified when applied to

radionuclides with relatively short physical half-lives to account for the fact that physical decay will substantially reduce activity concentrations actually observed in biota. Although the adoption of factors to modify CRs might be applicable to the present case in which determinations for ^{131}I, ^{129m}Te, ^{110m}Ag and ^{89}Sr are needed, for the sake of simplicity and traceability the original CR values were applied. Because the factors used to modify CR values as applied to short-lived radionuclides are fractions of 1, the calculations made in the assessment can be considered conservative.

IV. SETTING UP THE DYNAMIC MODEL

21. The model described in the methodology was implemented in ECOLEGO (figure VII). Ecolego is a simulation software tool that is used for creating dynamic models and performing deterministic and probabilistic simulations [Avila et al., 2005].

Figure VII. Screenshot showing model configuration in ECOLEGO-6

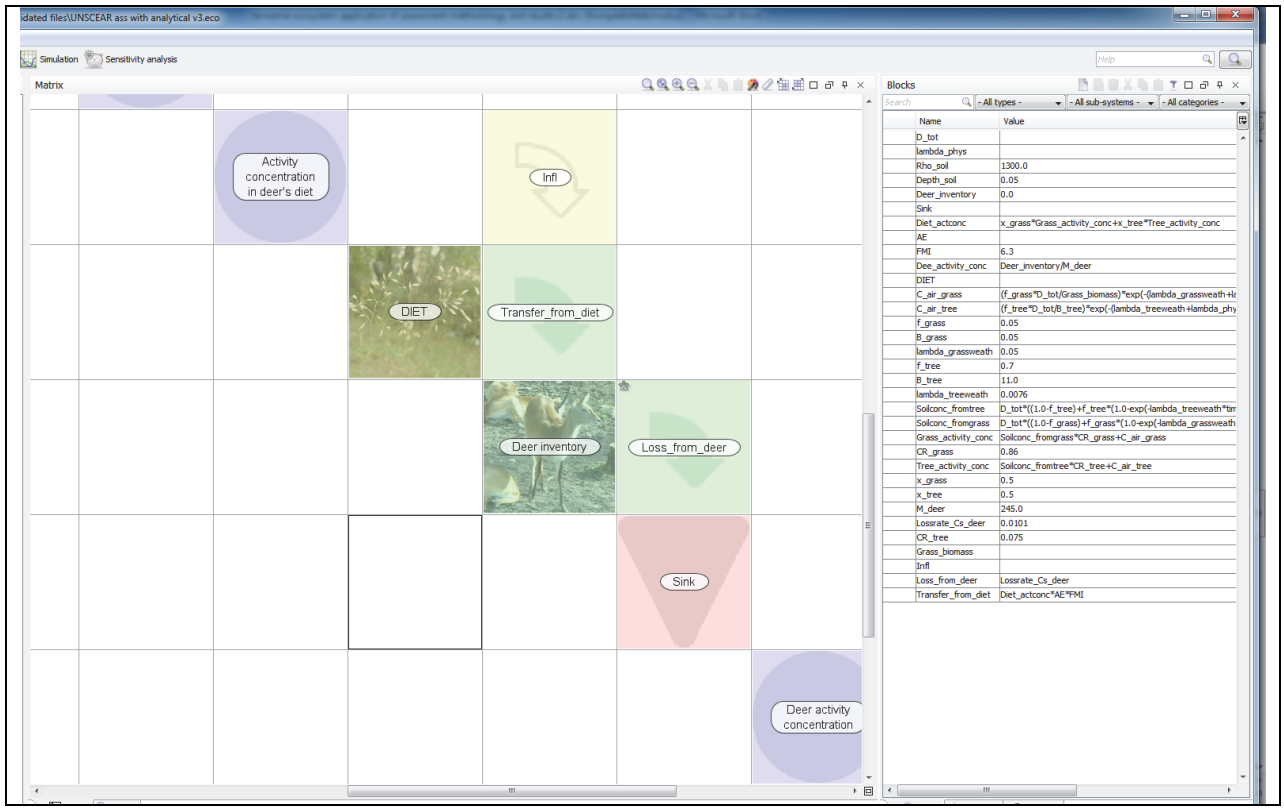

22. Initial focus was placed upon ^{137}Cs and mammal (deer) using the representative example of Sika deer.

23. Following exchanges with MEXT, it was clear that the MEXT data pertained to total deposition density and not just the component of deposition density associated with soil. They collected soil together with small weeds or other vegetation if there were any and also collected root zones as soil samples. The model was run using a deposition density of 1 kBq/m^2.

~~IV.~~V. RESULTS

(a) Detailed assessment with direct measurements in animals

24. Dose rates derived for all wild boar clusters were in the range of 0.8 to 1.1 µGy/h with the dose primarily attributable to ^{137}Cs and ^{134}Cs. However, as mentioned earlier, owing to the limitation of data, the cluster appoach was restricted to wild boar only. To expand the dose assessment to include other organisms, the city of Koriyama was selected because of the availability of in situ data. Using deposition density and activity concentration data reported for this location as input into the ERICA Tool, estimates of dose rates for four species were made (see table 5). The derived total dose-rate values were based on the arithmetic mean and the range was generated by considering minimum and maximum values for both soil and biota. As seen from the results (table 5), the external exposure component of the dose rates dominates and caesium is the main contributor to the estimated dose rates, and ^{134}Cs has the higher share (figure VIII).

Table 5. Total weighted dose rates for wildlife in Koriyama city. Based on empirical data; deposition density and activity concentration (for caesium isotopes)

Species	*Total dose rate (µGy/h)*	*Range (µGy/h)*	*Contribution from external exposure (%)*	*Contribution of caesium to total dose rates (%)*
Wild boar	0.55	0.06–2.0	73	92
Asian black bear	0.57	0.13–1.9	65	93
Sika deer	0.50	0.08–1.9	78	91
Birds	0.7	0.03–2.8	94	95

Figure VIII. Estimated absorbed dose rates (µGy/h) for representative organisms in Koriyama. 'Others' includes radionuclides such as ^{131}I, ^{110m}Ag, ^{89}Sr and ^{90}Sr

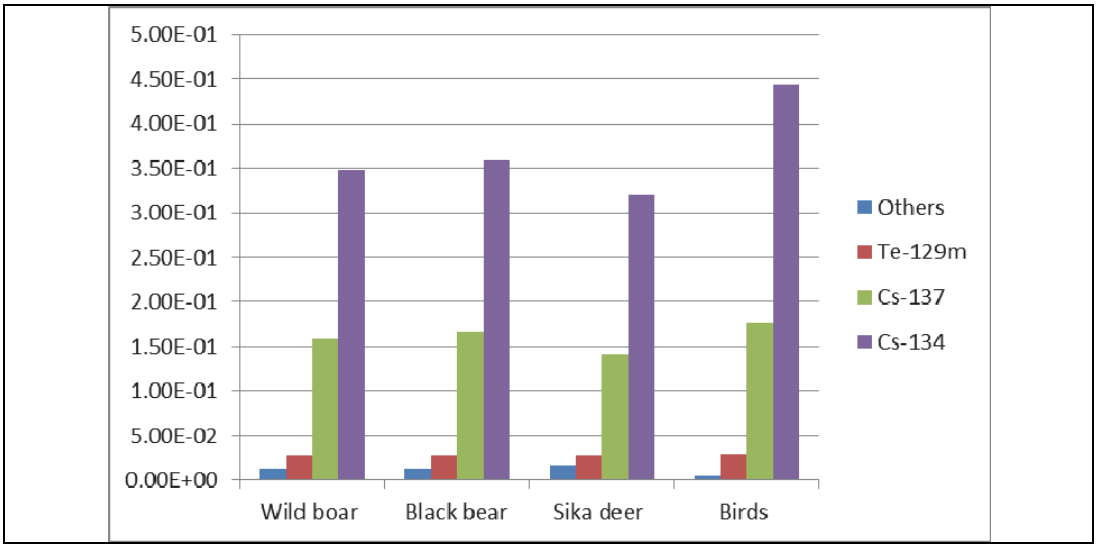

(b) Equilibrium assessment using maximum deposition density values

25. Weighted absorbed dose rates for selected organism groups using the maximum *(a)* reported and *(b)* decay-corrected activity concentrations from Okuma Town (table 3) are presented in figure IX. Because these calculations were based on data from a single

measurement point, they were considered to provide only a highly uncertain indication of upper percentile exposure rates for plants and animals in the accident-affected region.

26. For exposure estimates based upon maximum deposition density levels at the reference date in July 2011, the highest weighted absorbed dose rate of approximately 400 μGy/h was estimated for deer/herbivorous mammal. A large fraction of this dose rate was due to radioisotopes of caesium (^{134}Cs = 61 % and ^{137}Cs = 35 % of total weighted absorbed dose rate) and to internal exposure (approximately 88 %). Exposure estimates for vegetation at the reference date were substantially lower than those determined for mammals, falling at levels of 100 and 140 μGy/h for pine tree and grass, respectively.

27. The maximum weighted absorbed dose rates estimated by accounting for the physical decay of short-lived radionuclides between the time of primary deposition and sampling were considerably greater (by a factor of 2–3 times depending on organism type) than exposures determined at the reference date. For the decay-corrected estimates, a highest weighted absorbed dose rate of approximately 600 μGy/h was calculated for deer/herbivorous mammal. The primary contribution to the exposure estimate was from internal exposure due to radioisotopes of caesium.

28. The validity of decay-correcting short-lived radionuclides to the time of deposition and then applying a CR to derive dose rate estimates for internal exposure is questionable because of the underlying assumption that instantaneous equilibration has occurred between activity concentrations in soil and biota. Nonetheless, the observations that *(a)* for the model as applied, external exposure appears to be an important component of exposure for all of the organisms considered, with the exception of deer/herbivorous mammal, and that *(b)* the time evolution of radionuclide activity concentrations in soil, upon which external exposure is assessed, is dictated primarily by physical decay processes, mitigate this potentially confounding feature of the analysis.

29. The exposure estimates based on arithmetic mean of the deposition density levels for the areas of highest deposition density (table 3) provide a more reliable, less uncertain, indication of upper percentile dose rates for plants and animals in the accident-affected region because values are based upon more samples and are, therefore, supported by better underlying statistics. Furthermore, the data used provide a more representative indication of deposition density over an area that might feasibly be considered as harbouring viable populations of biota. Weighted absorbed dose rates for selected organism groups using the arithmetic *(a)* reported and *(b)* decay-corrected activity concentrations from Okuma Town (Table 3) are presented in figure X.

30. The maximum weighted absorbed dose rates associated with the calculations made for the reference date were determined for deer/herbivorous mammal and amounted to 71 μGy/h (or 1.7 mGy/day). Virtually the entire dose rate (99 %) was due to radioisotopes of caesium and internal exposure predominated (figure X(c)). Somewhat lower weighted absorbed dose rates were determined for vegetation, with exposures of 26 μGy/h and 17 μGy/h estimated for grass and trees respectively.

Figure IX. a) Weighted absorbed dose rate for selected biota based on maximum reported deposition densities in soils at Okuma Town, blue solid bars = dose rates based on reported activity concentrations at reference date and yellow striped bars = dose rates based on activity concentrations, decay-corrected to 15 March 2011. Radionuclide and internal/external contribution to total weighted absorbed dose rates for mammal at b) time of maximum deposition (decay-corrected to 15 March 2011) and c) reference date

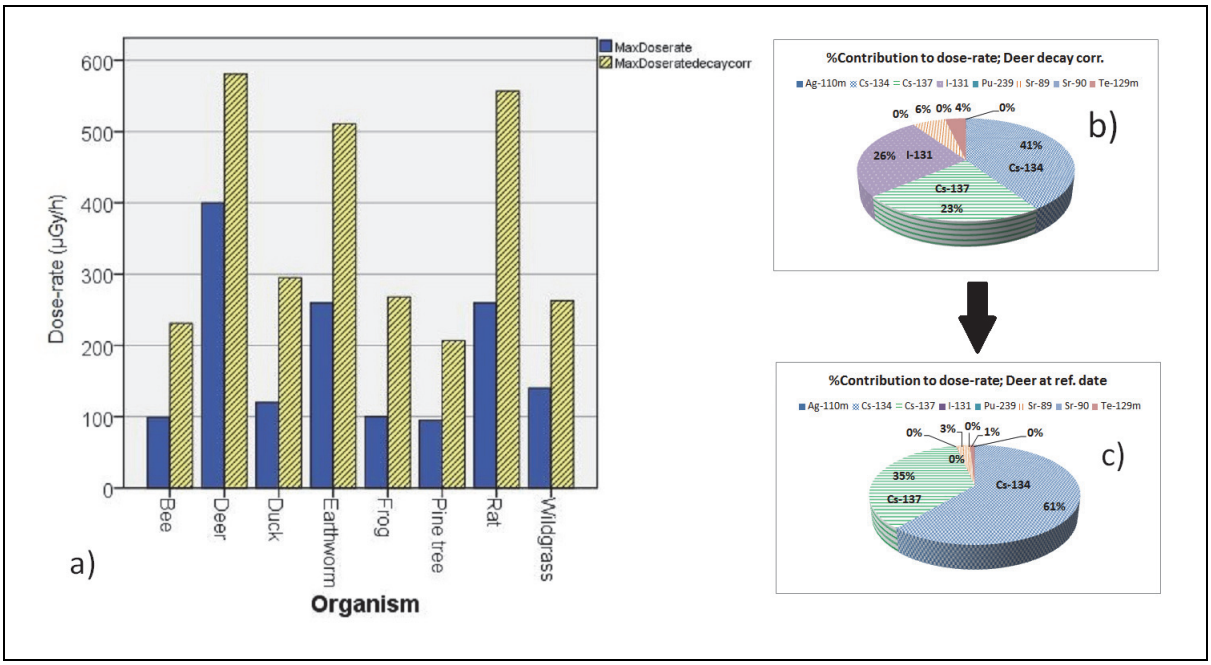

Figure X. a) Weighted absorbed dose rate for selected biota based on average reported deposition density in soils at Okuma Town, blue solid bars = dose rates based on reported activity concentrations at reference date, yellow striped bars = dose rates based on activity concentrations decay-corrected to 15 March 2011. Radionuclide and internal/external contribution to total weighted absorbed dose rates for deer/herbivorous mammal at b) time of maximum deposition (decay-corrected to 15 March 2011) and c) reference date

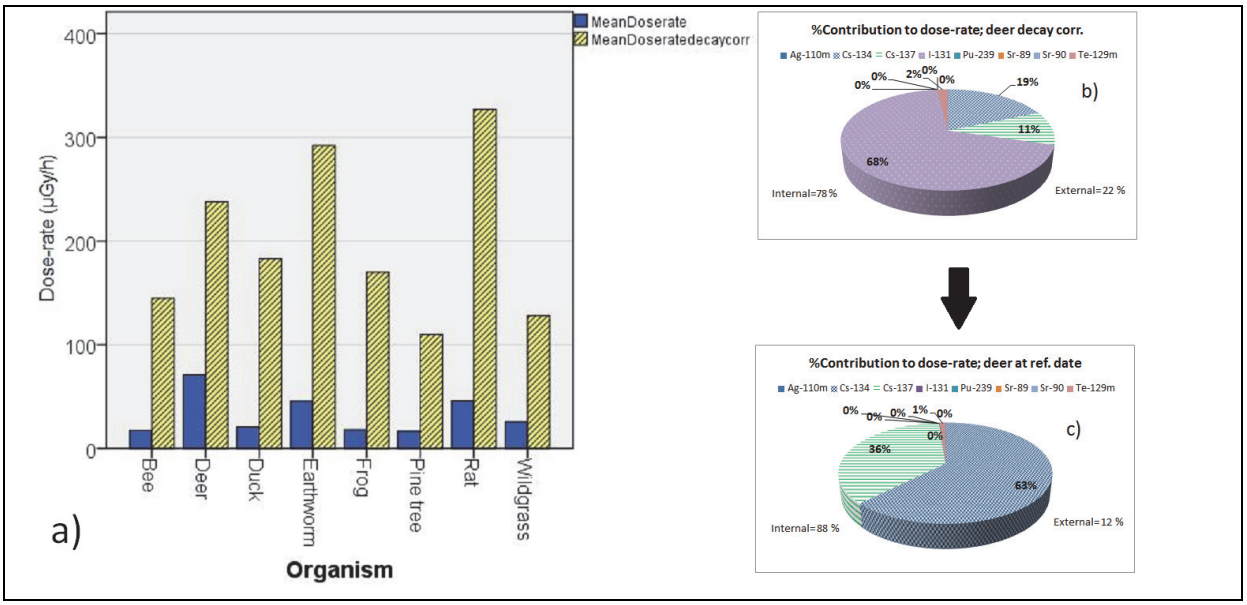

31. When the radioactive decay of short-lived radionuclides was accounted for, the estimated weighted absorbed dose rates at the time of the assumed main deposition event increased substantially. Maximum exposures were then calculated to be associated with soil-

dwelling organisms with derived dose rates of 290 µGy/h and 330 µGy/h for earthworm/soil invertebrate and rat/burrowing mammal respectively.

32. Weighted absorbed dose rates for deer/herbivorous mammal were estimated to be 240 µGy/h with ^{131}I and internal exposure making dominant contributions to this exposure (figure X (b)). In contrast, the external exposure predominated for all other organisms considered. Calculated dose rates for vegetation fell in the range 110 to 130 µGy/h.

(c) Dynamic modelling predictions

33. Model predictions for activity concentrations of ^{137}Cs in grass, tree and deer following a deposition of 1 kBq/m^2 are presented in figure XI. Because the modelled activity concentrations in deer exhibit a linear response to deposition, predictions can be easily made for any given deposition by applying a correction factor based on the relative magnitude of the deposition to 1 kBq/m^2.

Figure XI. Changes in ^{137}Cs activity concentration with time followin an initial deposition of 1 kBq m^{-2}. Light green squares and solid line =^{137}Cs in grass (Bq/kg f.w.); dark green circles and broken line = ^{137}Cs in tree (Bq/kg f.w.); red triangles and dashed line = ^{137}Cs in deer (Bq/kg f.w.)

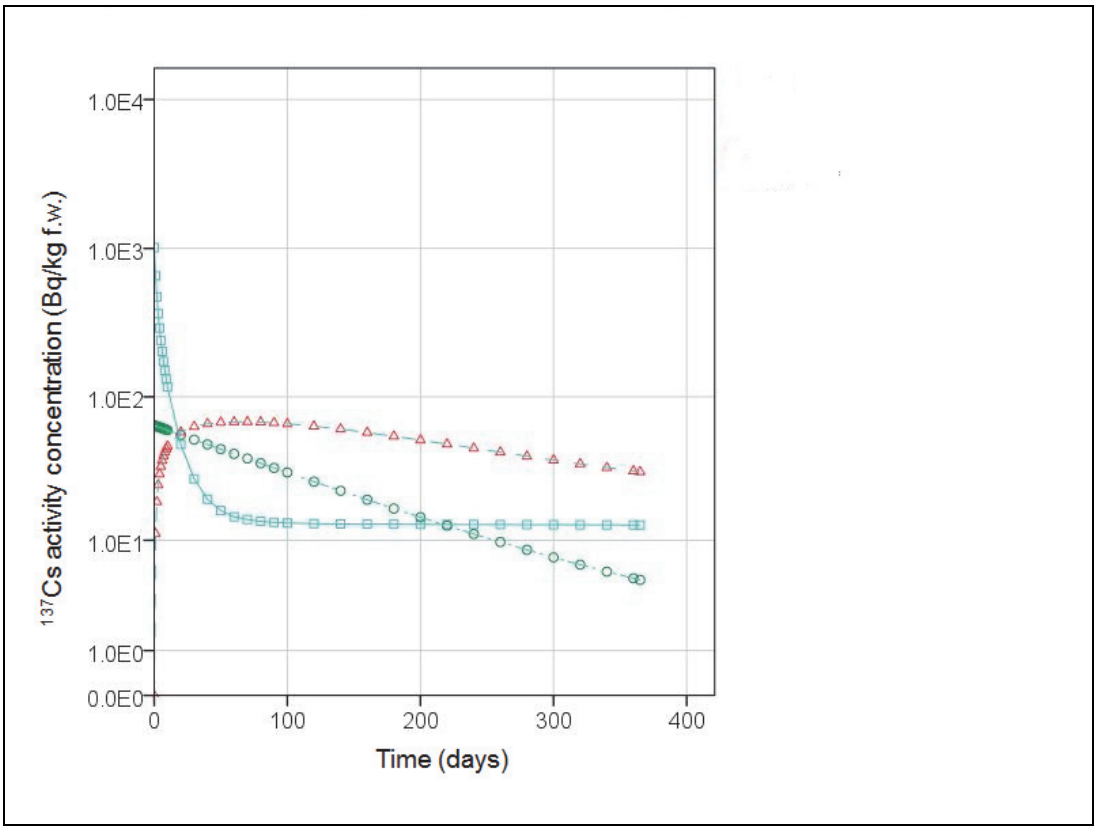

34. Activity concentrations in grass fell rapidly, reflecting the relatively high weathering rates and biomass dilution associated with the start of the growing season, falling from a maximum activity concentration of approximately 1000 Bq/kg f.w. to levels slightly in excess of 10 Bq/kg f.w. within the first 50 days or so after deposition. Initial activity concentrations in trees were approximately 60 Bq/kg f.w. but lower weathering rates led to a much slower decline in activity concentrations with time compared to grass and falling to levels below 10 Bq/kg f.w. approximately 250 days after deposition. Modelled activity concentrations in deer increased for the initial 65 days after deposition attaining a maximum activity

concentration of ca. 70 Bq/kg f.w before declining gradually to levels around 30 Bq/kg f.w. 1 year after deposition.

35. In the process of initial model testing, paired samples of deposition density on soil and activity concentration for Sika deer of ^{137}Cs were selected. The simplest way to do this was to select the deposition density sample nearest to the location of the animal sampling to provide a corresponding pair. The dynamic model was then run using the deposition density data and estimates made for ^{137}Cs concentration in deer for comparison with the empirical data pertaining to Sika deer. The starting date for the model was taken to be 15 March 2011, assuming that the deposition occurred in one discrete event at this time. The time for estimation was thereafter selected as the time when the deer sample was taken. Therefore, 15 November 2011 would correspond to an estimate for eight months after deposition.

36. The comparison between modelled (predicted) and measured values is provided in figure XII.

Figure XII. Predicted versus measured activity concentrations of ^{137}Cs in (Sika) deer; the measured data include 2 values below detection limits (where activity concentrations were assumed to be at the detection limit)

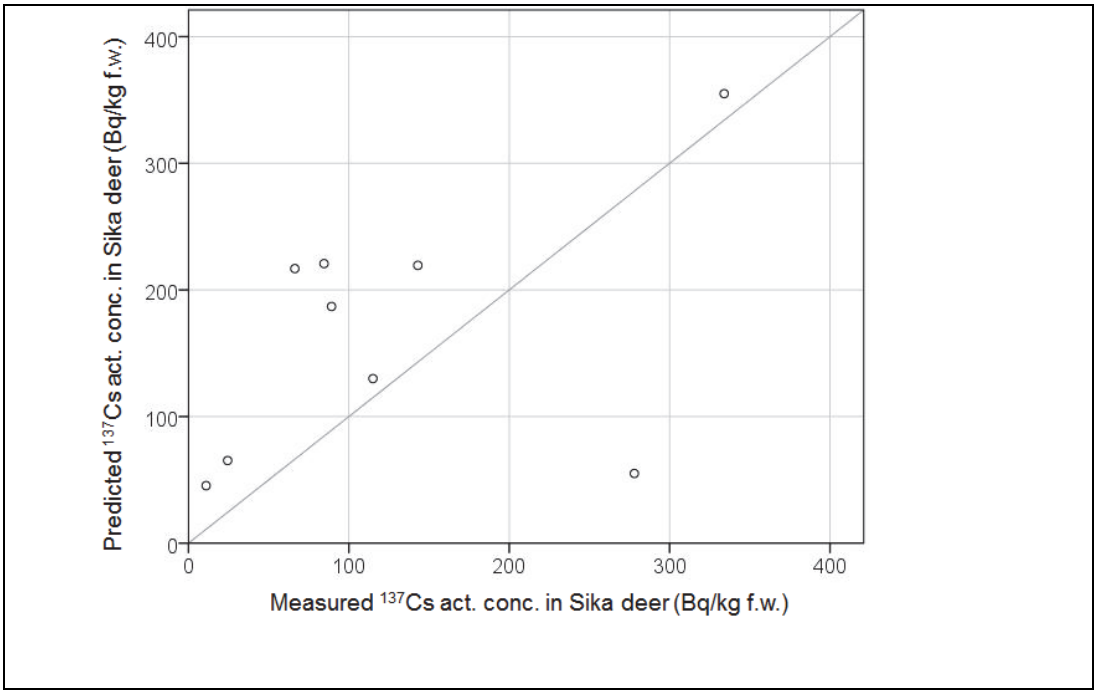

37. In view of the large uncertainties associated with numerous parameters adopted within the model implementation, especially those characterizing activity levels within the diet of Sika deer, the predictions were quite reasonable. The model appeared to have a slight tendency to over-estimate activity concentrations but by no more than a factor of approximately 2. In only one case was there a substantial under-estimation for which the modelled value was a factor of approximately 5 below the measurement.

38. Dose rates arising from ^{134}Cs, ^{137}Cs and ^{131}I were calculated using the arithmetic mean of the deposition density data for Okuma Town (figure XIII). The deposition density levels for ^{131}I were decay-corrected to 15 March 2011. This might be considered as a hypothetical exercise, because the presence of Sika deer in the Okuma Town area had not been established. Nonetheless, the dose rates might be considered as indicative of exposures for any deer-sized herbivorous mammal present in this area.

Figure XIII. Dose rates versus time for (i) grass: light green squares, solid lines, (ii) tree: dark green circles broken line and (iii) deer: red triangles and dashed line

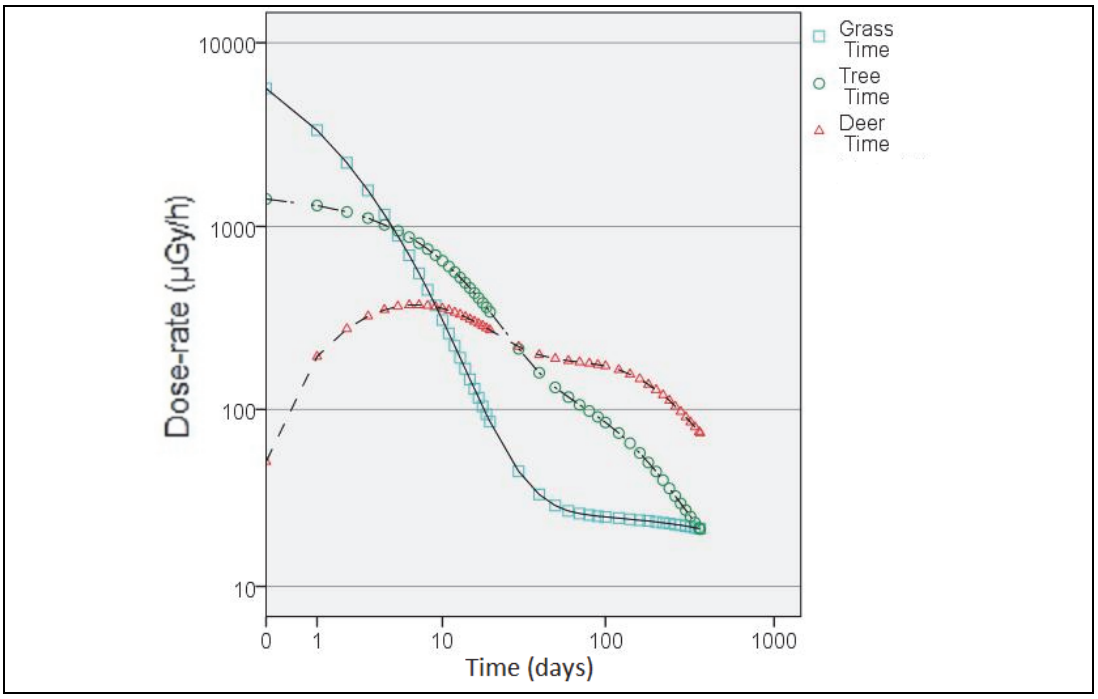

39. Highest weighted absorbed dose rates were estimated for grass, with levels of approximately 5.6 mGy/h at the time of deposition. A large fraction of this original dose rate (>85%) was due to ^{131}I present on the vegetation surfaces and modelled most appropriately as an internal exposure. The dose rates for grass decreased rapidly, falling to levels below 100 µGy/h in the 15 days following deposition. The accumulated dose in the first 30 days after deposition slightly exceeded 0.45 Gy. Weighted absorbed dose rates for trees were initially at a substantially lower level than those modelled for grass with exposures of about 1.4 mGy/h. However, dose rates declined less rapidly than those for grass and were estimated not to have fallen below 100 µGy/h until about 80 days of elapsed time following deposition. The main contribution to dose, as for grass, was due to ^{131}I on vegetation. The accumulated dose in the first 30 days was commensurate with the value estimated for grass, falling just below 0.45 Gy. Maximum dose rates for deer/herbivorous mammals were estimated to have occurred within the first week following the main deposition event attaining dose rates of 370 µGy/h. A large fraction of this initial dose rate (64%) was associated with internal exposure due to ^{131}I. Although dose rates fell quite rapidly, with levels below 200 µGy/h following 40 days of simulation time, dose rates did not fall below 100 µGy/h until time=275 days. The accumulated dose in the first month following the accident was estimated to be approximately 0.2 Gy.

40. The initial, maximum dose rates estimated for vegetation resulting from the dynamic modelling approach were quite different from values derived using an equilibrium-based approach even when decay was accounted for in the latter. This could be quite clearly seen for grass where the dynamic approach predicted dose rates exceeding the equilibrium-based estimate by a factor of approximately 44. This discrepancy was even more apparent if consideration is given to the fact that the equilibrium simulation included a broader suite of radionuclides. For deer/herbivorous mammals, the discrepancy between the models was less pronounced, although the dynamic model still produced estimates that fell a factor of 1.6 above the decay-corrected equilibrium-based model when exposures were at a maximum. For all organisms, over the first few months the absorbed dose rates estimated using the two approaches converged and thereafter the dynamic model produced lower dose-rate estimates

than the equilibrium model (presumably reflecting the decay of ^{131}I being accounted for in the former model).

References

Avila R., R. Broed and A. Pereira. ECOLEGO - A toolbox for radioecological risk assessment. pp. 229–232 in: Proceedings of the International Conference on the Protection from the Effects of Ionizing Radiation. IAEA-CN-109/80. International Atomic Energy Agency, Vienna (2005).

Brown, J.E., B. Alfonso, R. Avila et al. The ERICA Tool. J. Environ. Radioact. 99(9): 1371-1383 (2008).

Clark, P.J. and F.C. Evans. Distance to nearest neighbour as a measure of spatial relationships in populations. Ecology 35: 445-453 (1954).

Donnelly, K. Simulations to determine the variance and edge-effect of total nearest neighbour distance. pp. 91-95 in: Simulation Methods in Archaeology. Cambridge University Press, 1978.

Fukushima Prefecture. Radiation monitoring data of wildlife in Fukushima prefecture. [Internet] Available from (http://www.pref.fukushima.lg.jp/sec/16035b/wildlife-radiationmonitoring1.html) on 5 February 2013. (Japanese).

Gribov, A. and K. Krivoruchko. new flexible non-parametric data transformation for trans-Gaussian Kriging. Geostatistics Oslo 2012. pp. 51-65 in: Quantitative Geology and Geostatistics, Volume 17, Part 1. Springer, Netherlands, 2012.

Hamershock, D.M., T.W. Seamans and G.E. Bernhardt. Determination of body density for twelve bird species. Report to the National Technical Information Service, Flight Dynamics Directorate, Wright Laboratory AFMC (1993).

IAEA. Handbook of parameter values for the prediction of radionuclide transfer in terrestrial and freshwater environments. IAEA-TRS-472. IAEA, Vienna (2010).

ICRP. Environmental protection: Transfer parameters for reference animals and plants. ICRP Publication 114. Annals of the ICRP 39(6). International Commission on Radiological Protection, Oxford, 2009.

Kaufman, L. and P.J. Rousseeuw. Finding Groups in Data: An Introduction to Cluster Analysis. Wiley-Interscience, 2005.

Krivoruchko, KSpatial Statistical Data Analysis for GIS Users. Esri Press, Redlands, CA, 2011.

Pilz, J., H. Kazianka and G. Spöck. Some advances in Bayesian spatial prediction and sampling design. Spatial Statistics 1: 65-81 (2012).

Yasunari, T.J., A. Stohl, R.S. Hayano et al. Cesium-137 deposition and contamination of Japanese soils due to the Fukushima nuclear accident. PNAS 108(49): 19530-19534 (2011).

Yoshida, N. and Y. Takahashi. Land-surface contamination by radionuclides from the Fukushima Daiichi nuclear power plant accident. Elements 8(3): 201-206 (2012).